



A New Electrically Conducting Metal–Organic Framework Featuring U-Shaped *cis*-Dipyridyl Tetrathiafulvalene Ligands

Monica A. Gordillo, Paola A. Benavides, Kaybriana Spalding and Sourav Saha*

Department of Chemistry, Clemson University, Clemson, SC, United States

A new electrically conducting 3D metal-organic framework (MOF) with a unique architecture was synthesized using 1,2,4,5-tetrakis-(4-carboxyphenyl)benzene (TCPB) a redox-active *cis*-dipyridyl-tetrathiafulvalene (Z-DPTTF) ligand. While TCPB formed $Zn_2(COO)_4$ secondary building units (SBUs), instead of connecting the Zn_2 -paddlewheel SBUs located in different planes and forming a traditional pillared paddlewheel MOF, the U-shaped Z-DPTTF ligands bridged the neighboring SBUs formed by the same TCPB ligand like a sine-curve along the b axis that created a new *sine*-MOF architecture. The pristine *sine*-MOF displayed an intrinsic electrical conductivity of 1×10^{-8} S/m, which surged to 5×10^{-7} S/m after I_2 doping due to partial oxidation of electron rich Z-DPTTF ligands that raised the charge-carrier concentration inside the framework. However, the conductivities of the pristine and I_2 -treated *sine*-MOFs were modest possibly because of large spatial distances between the ligands that prevented π -donor/acceptor charge-transfer interactions needed for effective through-space charge movement in 3D MOFs that lack through coordination-bond charge transport pathways.

Keywords: metal-organic frameworks, redox-active, tetrathiafulvalene, electrical conductivity, iodine

OPEN ACCESS

Edited by:

Himanshu Sekhar Jena,
Ghent University, Belgium

Reviewed by:

Sasanka Dalapati,
Central University of Tamil Nadu, India
Deanna D'Alessandro,
The University of Sydney, Australia

*Correspondence:

Sourav Saha
souravs@clemson.edu

Specialty section:

This article was submitted to
Inorganic Chemistry,
a section of the journal
Frontiers in Chemistry

Received: 17 June 2021

Accepted: 09 September 2021

Published: 01 October 2021

Citation:

Gordillo MA, Benavides PA, Spalding K
and Saha S (2021) A New Electrically
Conducting Metal–Organic Framework
Featuring U-Shaped *cis*-Dipyridyl
Tetrathiafulvalene Ligands.
Front. Chem. 9:726544.
doi: 10.3389/fchem.2021.726544

INTRODUCTION

Metal organic frameworks (MOFs) are versatile materials with diverse structures, composition, properties, and functions (Furukawa et al., 2013; Yuan et al., 2018). These characteristics of MOFs have attracted researchers because of their potential applications in catalysis (Liu et al., 2014; Dolgoplova and Shustova, 2016), guest separation (Li et al., 2012), storage (Sumida et al., 2012), and delivery, light harvesting (Zhang and Lin, 2014; Liu et al., 2015; So et al., 2015; Maza et al., 2016; Gordillo et al., 2019), ionic and electronic conduction (Horike et al., 2013; Ramaswamy et al., 2014; Stavila et al., 2014; Sun et al., 2016; Stassen et al., 2017), and sensing (D'Alessandro, 2016; Lustig et al., 2017; Khatun et al., 2019), among other advanced applications (Rice et al., 2020). Introducing redox-active ligands is a rather simple way to elicit multifunctionality in MOFs, a strategy that has been widely adopted in recent years (Ding et al., 2021). One of the most commonly used redox-active ligands is tetrathiafulvalene (TTF) (Segura and Martin, 2001; Canevet et al., 2009; Wang et al., 2017b), a sulfur containing electron-rich molecule that possesses two easily accessible redox states, i.e., TTF^{•+} radical cation and TTF²⁺ dication that has been widely employed as an electron donor in optoelectronic (Wang et al., 2017b), conductive (Narayan et al., 2012; Sun et al., 2016), and magnetic materials (Wang et al., 2017a). Equipped with two pyridyl groups on the TTF core, dipyridyl tetrathiafulvalene (DPTTF) ligand not only inherits the redox properties of parent TTF, but also becomes capable of coordinating

metal ions. The Z-DPTTF ligand, however, exists in a mixture of *E* and *Z*-isomers, with the latter surprisingly being the major isomer. The *E* isomer adopts a nearly linear shape, whereas the *Z*-isomer adopts a U-shape, which is probably one of the reasons why this ligand has not been as extensively incorporated in MOFs (Yin et al., 2016; Sherman et al., 2020; Weng et al., 2020) as other TTF derivatives (Park et al., 2015; Wang et al., 2015; Su et al., 2017; Wang et al., 2017a; Leong et al., 2018; Wang et al., 2019). Herein, we report the synthesis of a new electrically conducting *sine*-MOF $[\text{Zn}_2(\text{DPTTF})\text{TCPB}\bullet 3\text{DMA}]_n$ featuring 1,2,4,5-tetrakis-(4-carboxyphenyl)benzene (TCPB) and Z-DPTTF where the former formed $\text{Zn}_2(\text{COO})_4$ paddlewheel nodes while the latter connected the adjacent nodes formed by the same TCPB ligands via axial coordination in such a way that two U-shaped Z-DPTTF ligands axially coordinated to the same Zn_2 paddlewheel node completed a *sine*-wave propagating along the b-axis. This new *sine*-MOF displayed a 50-fold increase in room temperature electrical conductivity from 1×10^{-8} to 5×10^{-7} S/m after I_2 doping largely due to partial oxidation of the electron rich Z-DPTTF ligands, which enhanced the charge-carrier concentration.

EXPERIMENTAL SECTION

Materials

Reagents, starting materials, and solvents were purchased from Sigma-Aldrich, Acros Organic, TCI America and EMD Chemicals and used as received. Z-DPTTF ligand was prepared following a literature protocol (Han et al., 2007).

Preparation of *sine*-MOF

To a solution of Z-DPTTF ligand (7.2 mg, 0.02 mmol) in DMAc (2 ml) placed in a screw-capped vial, a separately prepared solution of $\text{Zn}(\text{NO}_3)_2\bullet 6\text{H}_2\text{O}$ (11.9 mg, 0.04 mmol) and TCPB (11.2 mg, 0.02 mmol) in 2:1 DMAc/ H_2O mixture (1.5 ml) was added slowly. Once all these starting materials were fully dissolved upon gentle shaking, 1 M HNO_3 ethanolic solution (20 μl) was added to it. The resulting mixture was then heated in an oven at 80°C for 24 h. The resulting dark-red crystals (48%) were used for single-crystal x-ray diffraction (SXRD) analysis and the corresponding evacuated powder was used for electrical and optical measurements. Elemental analysis: Calc. for $\text{Zn}_2\text{C}_{52}\text{H}_{37}\text{O}_{10.5}\text{S}_4\text{N}_2$: C 55.92, H 3.34, and S 11.48%. Found: C 56.01, H 3.44, and S 11.53%

Preparation of I_2 Doped *sine*-MOF

The dark-red colored evacuated *sine*-MOF powder was placed in a small open vial, which was then placed inside a larger screw-capped vial containing few I_2 chips. The larger vial was capped tightly and sealed with parafilm tape to keep the *sine*-MOF crystals exposed to iodine vapor for 3 days, which caused the *sine*-MOF powder to turn black. The I_2 -treated *sine*-MOF vial was removed from the I_2 chamber, left open overnight, and finally washed thoroughly with hexane until the washing solution became colorless indicating that the material was free of any physisorbed I_2 . Elemental analysis: Calc. for $\text{Zn}_2\text{C}_{55}\text{H}_{50}\text{O}_{14}\text{S}_4\text{N}_{2.5}\text{I}_{1.5}$: C 46.77, H 3.57, S 9.08%, and I 13.48%. Found: C 46.97, H 2.80, S 8.24, and I 13.44%.

RESULTS AND DISCUSSION

Synthesis, Structural Characterization, and Thermogravimetric Analysis of *sine*-MOF

A solvothermal reaction between $\text{Zn}_2(\text{NO}_3)_2\bullet 6\text{H}_2\text{O}$, TCPB, and Z-DPTTF in a DMAc/ H_2O mixture at 80°C for 24 h yielded dark-red *sine*-MOF crystals. SXRD analysis revealed that *sine*-MOF $[\text{Zn}_2(\text{DPTTF})\text{TCPB}\bullet 3\text{DMA}]_n$ crystallized in an orthorhombic space group Pnma (Figures 1A,B and Supplementary Figure S1). The TCPB ligands formed $\text{Zn}_2(\text{COO})_4$ paddlewheel nodes, but unlike typical pillared paddlewheel MOFs, they did not form 2D sheets of these nodes in *sine*-MOF. Instead, they formed a 3D framework thanks to a significant twist of TCPB ligand, which was evident from large dihedral angles (ca. $43\text{--}47^\circ$) between the central benzene ring and terminal benzoate rings. The axial sites of the $\text{Zn}_2(\text{COO})_4$ paddlewheel nodes were occupied by Z-DPTTF ligands, although these dipyriddy ligands did not act as typical pillars found in pillared paddlewheel MOFs. Instead, each U-shaped Z-DPTTF ligand bridged two adjacent Zn_2 nodes formed by two 1,3-benzoate groups of the same TCPB ligand. Each Zn_2 paddlewheel node carried one U-shaped Z-DPTTF ligand at the top axial position and another at the bottom axial position, which then bridged two adjacent Zn_2 nodes from the top and bottom axial positions, respectively. Thus, the consecutive Zn_2 nodes located along the b-axis were connected by U-shaped Z-DPTTF ligands in an alternating top/bottom fashion that resembled a full sine-wave (Figure 1C), prompting us to label this new architecture as *sine*-MOF. The formation of this uncommon architecture was made possible by the bent geometry of Z-DPTTF ligands having an angle of 36° between the two dithiolene rings and a dihedral angle of 10° between two *cis*-pyridyl rings. The bent geometry and short central C=C bond length (1.34 Å) of Z-DPTTF indicated that they existed in the neutral form in pristine *sine*-MOF (Gao et al., 2014; Su et al., 2017). Due to an alternate up/down orientation of Z-DPTTF ligands, *sine*-MOF lacks intermolecular $\pi\text{--}\pi$ and S $\bullet\bullet$ S interactions between the TTF cores, but it enjoys $\pi\text{--}\pi$ interaction between the dithiolene rings of Z-DPTTF and two benzoate rings of TCPB ligand that have a centroid-to-centroid distance of 3.66 Å (Supplementary Figure S2).

The experimental powder X-ray pattern (PXRD) of pristine *sine*-MOF was consistent with the simulated one obtained from the SXRD analysis, which confirmed the phase purity and crystallinity of the evacuated bulk material (Figure 2). Iodine is a mild oxidant that is known to chemically oxidize TTF and other electron rich π -systems (Su et al., 2017; Gordillo et al., 2020). Exposure of pristine *sine*-MOF crystalline powder to I_2 -vapors afforded a black material that was washed thoroughly with hexanes until the wash solution became colorless indicating that no residual physisorbed I_2 was left in the I_2 -treated *sine*-MOF. The PXRD pattern of the I_2 -treated *sine*-MOF matched with that of the pristine material, confirming the retention of its structural integrity and crystallinity (Supplementary Figure S3).

Thermogravimetric analysis (TGA) was performed on vacuum-dried pristine and I_2 -treated *sine*-MOF samples in N_2 atmosphere (Figure 3). The TGA profile of pristine *sine*-MOF revealed a gradual 10% weight loss until 300°C corresponding to the loss of solvent molecules, followed by a sharp 33% weight loss due to framework decomposition. The TGA profile of the I_2 -doped *sine*-MOF displayed an initial weight loss of 14%

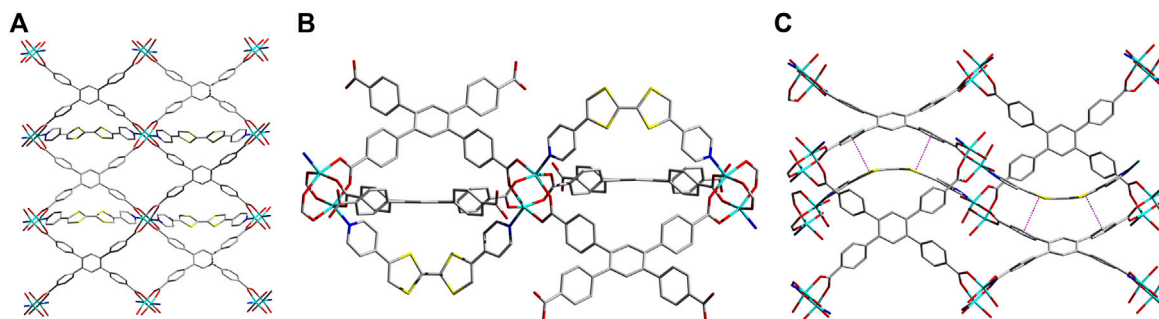


FIGURE 1 | (A) Crystal structure of *sine*-MOF $[Zn_2(DPTTF)TCPB \cdot 3DMA]_n$ viewed along the *c* axis. **(B)** The paddlewheel-like SBUs formed by the TCPB ligands are connected by axially coordinated U-shaped Z-DPTTF ligands extended along the *b*-axis. **(C)** A view of the sinusoidal thread formed by Z-DPTTF ligands by bridging adjacent SBU units along the *b* axis and the π - π interactions between the dithiolenes rings of the TTF core and two benzoate moieties of the TCPB ligand with a centroid-to-centroid distance of 3.66 Å. Solvent molecules and H atoms are omitted for clarity. Atom legends: cyan, Zn(II); blue, N; red, O; yellow, S; and gray, C.

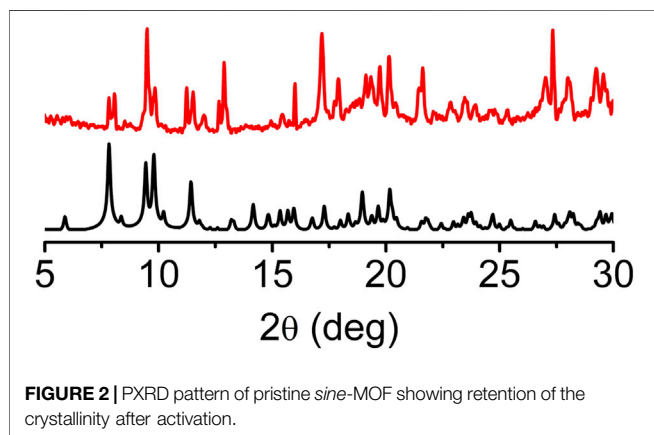


FIGURE 2 | PXRD pattern of pristine *sine*-MOF showing retention of the crystallinity after activation.

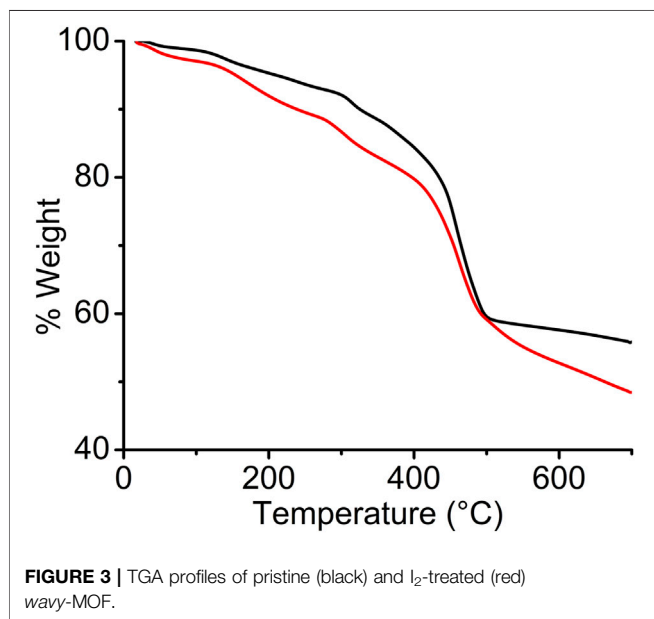


FIGURE 3 | TGA profiles of pristine (black) and I_2 -treated (red) *wavy*-MOF.

corresponding to the loss of MeOH and water molecules, followed by another significant weight loss step above 400°C that corresponded to framework decomposition.

Optical and Electrochemical Properties of *sine*-MOF

The diffuse reflectance spectra (DRS) of pristine and I_2 -doped *sine*-MOFs were measured. Pristine *sine*-MOF displayed a broad band centered on 480 nm, which was ca. 60 nm red-shifted with respect to the UV-vis absorption spectrum (λ_{max}) of Z-DPTTF recorded in DMF (**Figures 4A,B**). From the onset of the λ_{max} peak of the Z-DPTTF ligand its optical bandgap of 2.3 eV was calculated. The optical bandgaps of pristine and I_2 -treated *sine*-MOFs ($E_g = 1.8$ and 1.2 eV, respectively) (**Figure 4B**) were narrower than that of the free ligand, probably because of π - π and π -donor/acceptor interactions between the Z-DPTTF and TCPB ligands in pristine and I_2 -treated *wavy* MOFs, respectively. The results from the corresponding Tauc plot (**Figure 4C**) were in good agreement with those determined from DRS and revealed ~ 0.6 – 0.7 eV narrower bandgap for the I_2 -doped *sine*-MOF with respect to the pristine MOF. The narrower bandgap of I_2 -treated *sine*-MOF is likely due to a partial oxidation of the Z-DPTTF ligands to Z-DPTTF $^{\bullet+}$ radical cations within the framework.

Solid state cyclic voltammetry (CV) (**Figure 5**) and square wave voltammetry (SWV) (**Supplementary Figure S4**) were used to investigate the redox properties of *sine*-MOF. TTF compounds are known to display two reversible one electron oxidation steps corresponding to TTF $^{\bullet+}$ and TTF $^{2+}$ formation. The CV of pristine *sine*-MOF displayed two quasi-reversible oxidation processes (**Figure 5A**) with anodic peaks at 0.68 and 0.96 V (vs Ag/AgCl, 0.1 M Bu_4NPF_6 in MeCN) corresponding to stepwise one-electron oxidation of Z-DPTTF to Z-DPTTF $^{\bullet+}$ and Z-DPTTF $^{2+}$. The anodic peaks of I_2 -doped *wavy*-MOF (**Figure 5B**) appeared toward more positive potentials at 0.79 and 1.05 V suggesting that such I_2 -mediated partially oxidized framework was more difficult to oxidize electrochemically than pristine *sine*-MOF.

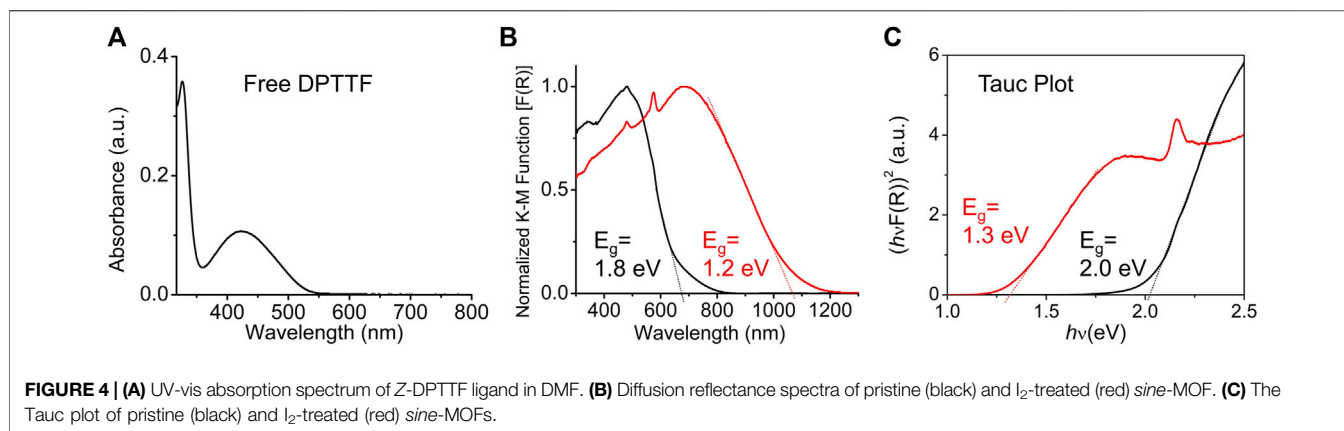


FIGURE 4 | (A) UV-vis absorption spectrum of Z-DPTTF ligand in DMF. (B) Diffusion reflectance spectra of pristine (black) and I₂-treated (red) *sine*-MOF. (C) The Tauc plot of pristine (black) and I₂-treated (red) *sine*-MOFs.

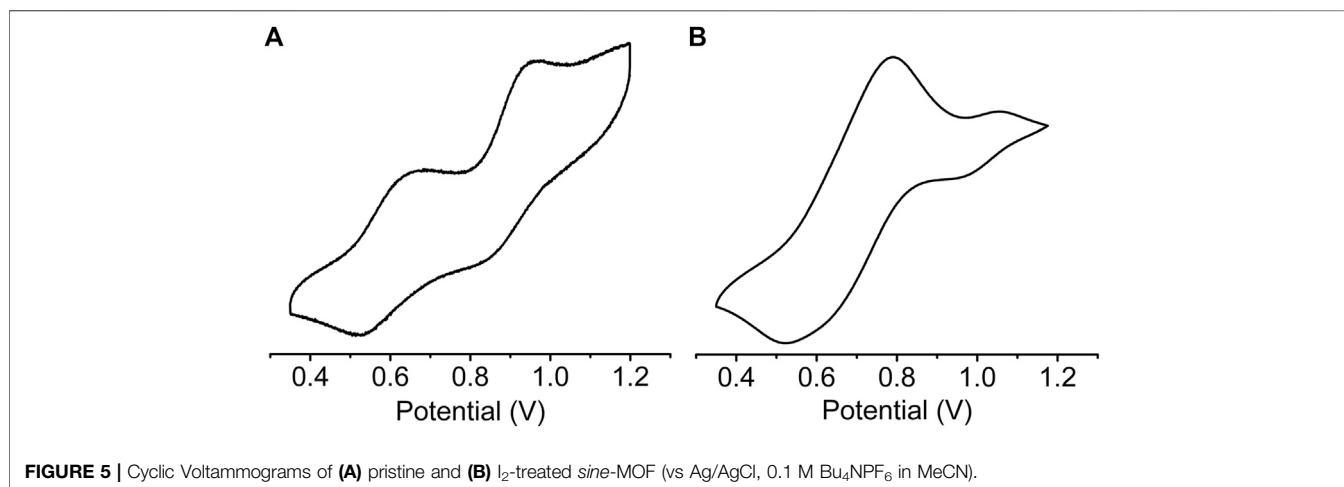


FIGURE 5 | Cyclic Voltammograms of (A) pristine and (B) I₂-treated *sine*-MOF (vs Ag/AgCl, 0.1 M Bu₄NPF₆ in MeCN).

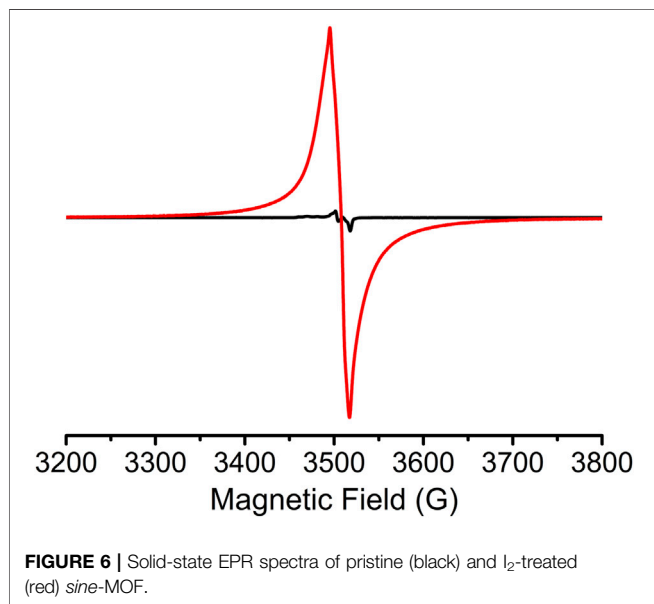
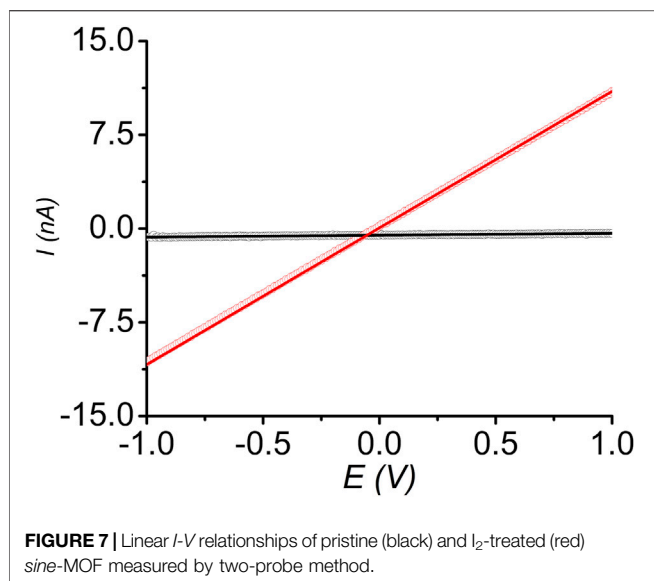


FIGURE 6 | Solid-state EPR spectra of pristine (black) and I₂-treated (red) *sine*-MOF.

Solid-state electron paramagnetic resonance (EPR) confirmed the presence of Z-DPTTF^{•+} radical cations within the *sine*-MOF. A weak EPR signal (Figure 6) was present in pristine *sine*-MOF

indicating that most of the Z-DPTTF ligands were in the neutral state and that a small percentage may have been oxidized by air as has been previously reported for other TTF-based MOFs. (Narayan et al., 2012; Park et al., 2015; Su et al., 2017; Wang et al., 2017a; Leong et al., 2018). In contrast, a strong EPR signal ($g \approx 2.006$) was observed (Figure 6) for I₂-treated *sine*-MOF indicating that a significant population of Z-DPTTF ligands were oxidized to paramagnetic Z-DPTTF^{•+} radical cations. The elemental analysis data of I₂-treated *sine*-MOF (*vide supra*) corresponded to an empirical formula of Zn₂C₅₅H₅₀O₁₄S₄N₂I_{1.5}. Based on the I/S ratio, we estimated that there was roughly one I₃⁻ anion for two DPTTF ligands (each DPTTF has four S atoms), meaning that approximately half of the DPTTF ligands were partially oxidized to DPTTF^{•+} radical cations, which were accompanied by an equal number of I₃⁻ counterions for charge balance. Furthermore, based on the empirical formula and quantitative EPR analysis, we estimated that the pristine *sine*-MOF possessed 6.8×10^{13} spins/mg or 7.6×10^{19} spins/mol, which corresponded to only 0.01% DPTTF^{•+} population (possibly produced by negligible aerobic oxidation). In contrast, the I₂-treated *sine*-MOF possessed 2.6×10^{16} spins/mg or 3.6×10^{22} spins/mol, which corresponded to a noticeably higher 6.1% DPTTF^{•+} population. Thus, elemental analysis and quantitative EPR analysis together helped us quantify the DPTTF^{•+} population in the I₂-treated partially oxidized *sine*-MOF.



Conductivity Measurements of Pristine and I_2 -Treated *sine*-MOFs

Finally, we measured the room temperature electrical conductivity of pressed pellets of pristine and I_2 -treated *sine*-MOFs, which provided us insights into the effect of partial oxidation of Z-DPTTF ligands in the latter. DC-sweep measurements of pressed *sine*-MOF-pellets sandwiched between two conductive stainless-steel electrodes coated with Ag paste were conducted. Both materials displayed linear current-voltage (I - V) responses between -1 and $+1$ V (Figure 7), confirming ohmic contact between the pellets and electrodes. From the slopes of the corresponding I - V curves, the electrical conductivity of pristine and I_2 -treated *sine*-MOFs was determined to be 1×10^{-8} and 5×10^{-7} S/m, respectively. The 50-fold higher conductivity of I_2 -treated *sine*-MOF was attributed to partial oxidation of Z-DPTTF ligands to Z-DPTTF $^{\bullet+}$, which enhanced the charge carrier concentration. However, the increase was modest and the conductivity was still lower than other I_2 -treated TTF-based MOFs possibly because *sine*-MOF lacked sufficient π - π or S $\bullet\bullet$ S interactions between the Z-DPTTF ligands, which hindered through-space charge movement, while the Zn_2 paddlewheel nodes were not conducive to through-bond charge movement. As result, pristine and I_2 -treated *sine*-MOFs likely relied on less effective charge hopping mechanism, which caused modest conductivities even though the latter possessed larger number of mobile charge carriers due to the presence of DPTTF $^{\bullet+}$ radical cations.

REFERENCES

- Canevet, D., Sallé, M., Zhang, G., Zhang, D., and Zhu, D. (2009). Tetrathiafulvalene (TTF) Derivatives: Key Building-Blocks for Switchable Processes. *Chem. Commun.* 17, 2245–2269. doi:10.1039/b818607n
- D'Alessandro, D. M. (2016). Exploiting Redox Activity in Metal-Organic Frameworks: Concepts, Trends and Perspectives. *Chem. Commun.* 52, 8957–8971. doi:10.1039/C6CC00805D

CONCLUSION

We have developed a new 3D *sine*-MOF structure featuring twisted TCPB ligands that formed $Zn_2(COO)_4$ paddlewheel nodes and axially coordinated U-shaped Z-DPTTF ligands that connected the adjacent nodes like sine-curves propagating along the b-axis. While the pristine *sine*-MOF displayed a modest intrinsic conductivity, its conductivity surged 50-fold to 5×10^{-7} S/m after iodine mediated partial oxidation of the electron rich Z-DPTTF ligands possibly due to enhanced charge carrier concentration. However, the lack of strong π - π - and S $\bullet\bullet$ S interactions between the Z-DPTTF ligands hindered through-space charge movement, which was largely reliant on charge hopping, causing modest electrical conductivity of both pristine and I_2 -treated *sine*-MOFs. These studies not only presented a novel electronic MOF architecture, but also demonstrated that a high charge carrier concentration alone is not sufficient for high electrical conductivity unless a framework is also equipped with effective charge transport pathways.

DATA AVAILABILITY STATEMENT

The CIF of the *sine*-MOF can be found in the Cambridge structural database with deposition number 2101676. The CIF and all the other additional data can also be found in the **Supplementary Material**.

AUTHOR CONTRIBUTIONS

SS conceived and supervised the project, evaluated data, and edited the article. MG, PB, and KS conducted experiments and analyzed data. MG also wrote the initial draft of the article.

FUNDING

This work was supported by the US National Science Foundation (award nos. DMR-1809092 and CHE-1660329) and Clemson University. KS was supported by NSF-REU award no. CHE-1560300.

SUPPLEMENTARY MATERIAL

The Supplementary Material for this article can be found online at: <https://www.frontiersin.org/articles/10.3389/fchem.2021.726544/full#supplementary-material>

- Ding, B., Solomon, M. B., Leong, C. F., and D'Alessandro, D. M. (2021). Redox-active Ligands: Recent Advances towards Their Incorporation into Coordination Polymers and Metal-Organic Frameworks. *Coord. Chem. Rev.* 439, 213891. doi:10.1016/j.ccr.2021.213891
- Dolgoplova, E. A., and Shustova, N. B. (2016). Metal-organic Framework Photophysics: Optoelectronic Devices, Photoswitches, Sensors, and Photocatalysts. *MRS Bull.* 41, 890–896. doi:10.1557/mrs.2016.246
- Furukawa, H., Cordova, K. E., O'Keeffe, M., and Yaghi, O. M. (2013). The Chemistry and Applications of Metal-Organic Frameworks. *Science* 341, 974–986. doi:10.1126/science.1230444

- Gao, F., Zhu, F.-F., Wang, X.-Y., Xu, Y., Wang, X.-P., and Zuo, J.-L. (2014). Stabilizing Radical Cation and Dication of a Tetrathiafulvalene Derivative by a Weakly Coordinating Anion. *Inorg. Chem.* 53, 5321–5327. doi:10.1021/ic5006117
- Gordillo, M. A., Benavides, P. A., Panda, D. K., and Saha, S. (2020). The Advent of Electrically Conducting Double-Helical Metal-Organic Frameworks Featuring Butterfly-Shaped Electron-Rich π -Extended Tetrathiafulvalene Ligands. *ACS Appl. Mater. Inter.* 12, 12955–12961. doi:10.1021/acsmi.9b20234
- Gordillo, M. A., Panda, D. K., and Saha, S. (2019). Efficient MOF-Sensitized Solar Cells Featuring Solvothermally Grown [100]-Oriented Pillared Porphyrin Framework-11 Films on ZnO/FTO Surfaces. *ACS Appl. Mater. Inter.* 11, 3196–3206. doi:10.1021/acsmi.8b17807
- Han, Y.-F., Zhang, J.-S., Lin, Y.-J., Dai, J., and Jin, G.-X. (2007). Synthesis and Characterization of Half-sandwich Iridium Complexes Containing 2,6(7)-Bis(4-Pyridyl)-1,4,5,8-Tetrathiafulvalene and Ancillary Ortho-Carborane-1,2-Dichalcogenolato Ligands. *J. Organomet. Chem.* 692, 4545–4550. doi:10.1016/j.jorganchem.2007.04.034
- Horike, S., Umeyama, D., and Kitagawa, S. (2013). Ion Conductivity and Transport by Porous Coordination Polymers and Metal-Organic Frameworks. *Acc. Chem. Res.* 46, 2376–2384. doi:10.1021/ar300291s
- Khatun, A., Panda, D. K., Sayresmith, N., Walter, M. G., and Saha, S. (2019). Thiazolothiazole-Based Luminescent Metal-Organic Frameworks with Ligand-To-Ligand Energy Transfer and Hg²⁺-Sensing Capabilities. *Inorg. Chem.* 58, 12707–12715. doi:10.1021/acs.inorgchem.9b01595
- Leong, C. F., Wang, C.-H., Ling, C. D., and D'Alessandro, D. M. (2018). A Spectroscopic and Electrochemical Investigation of a Tetrathiafulvalene Series of Metal-Organic Frameworks. *Polyhedron* 154, 334–342. doi:10.1016/j.poly.2018.07.023
- Li, J.-R., Sculley, J., and Zhou, H.-C. (2012). Metal-Organic Frameworks for Separations. *Chem. Rev.* 112, 869–932. doi:10.1021/cr200190s
- Liu, J., Chen, L., Cui, H., Zhang, J., Zhang, L., and Su, C.-Y. (2014). Applications of Metal-Organic Frameworks in Heterogeneous Supramolecular Catalysis. *Chem. Soc. Rev.* 43, 6011–6061. doi:10.1039/C4CS00094C
- Liu, J., Zhou, W., Liu, J., Howard, I., Kilbarda, G., Schlabach, S., et al. (2015). Photoinduced Charge-Carrier Generation in Epitaxial MOF Thin Films: High Efficiency as a Result of an Indirect Electronic Band Gap? *Angew. Chem. Int. Ed.* 54, 7441–7445. doi:10.1002/anie.201501862
- Lustig, W. P., Mukherjee, S., Rudd, N. D., Desai, A. V., Li, J., and Ghosh, S. K. (2017). Metal-organic Frameworks: Functional Luminescent and Photonic Materials for Sensing Applications. *Chem. Soc. Rev.* 46, 3242–3285. doi:10.1039/C6CS00930A
- Maza, W. A., Haring, A. J., Ahrenholtz, S. R., Epley, C. C., Lin, S. Y., and Morris, A. J. (2016). Ruthenium(II)-polypyridyl Zirconium(IV) Metal-Organic Frameworks as a New Class of Sensitized Solar Cells. *Chem. Sci.* 7, 719–727. doi:10.1039/c5sc01565k
- Narayan, T. C., Miyakai, T., Seki, S., and Dincă, M. (2012). High Charge Mobility in a Tetrathiafulvalene-Based Microporous Metal-Organic Framework. *J. Am. Chem. Soc.* 134, 12932–12935. doi:10.1021/ja3059827
- Park, S. S., Hontz, E. R., Sun, L., Hendon, C. H., Walsh, A., Van Voorhis, T., et al. (2015). Cation-Dependent Intrinsic Electrical Conductivity in Isostructural Tetrathiafulvalene-Based Microporous Metal-Organic Frameworks. *J. Am. Chem. Soc.* 137, 1774–1777. doi:10.1021/ja512437u
- Ramaswamy, P., Wong, N. E., and Shimizu, G. K. H. (2014). MOFs as Proton Conductors - Challenges and Opportunities. *Chem. Soc. Rev.* 43, 5913–5932. doi:10.1039/C4CS00093E
- Rice, A. M., Martin, C. R., Galitskiy, V. A., Berseneva, A. A., Leith, G. A., and Shustova, N. B. (2020). Photophysics Modulation in Photoswitchable Metal-Organic Frameworks. *Chem. Rev.* 120, 8790–8813. doi:10.1021/acs.chemrev.9b00350
- Segura, J. L., and Martin, N. (2001). New Concepts in Tetrathiafulvalene Chemistry. *Angew. Chem. Int. Ed.* 40, 1372–1409. doi:10.1002/1521-3773(20010417)40:8<1372:AID-ANIE1372>3.0.CO;2-I
- Sherman, D. A., Murase, R., Duyker, S. G., Gu, Q., Lewis, W., Lu, T., et al. (2020). Reversible Single crystal-to-single crystal Double [2+2] Cycloaddition Induces Multifunctional Photo-Mechano-Electrochemical Properties in Framework Materials. *Nat. Commun.* 11 (1), 1–10. doi:10.1038/s41467-020-15510-7
- So, M. C., Wiederricht, G. P., Mondloch, J. E., Hupp, J. T., and Farha, O. K. (2015). Metal-organic Framework Materials for Light-Harvesting and Energy Transfer. *Chem. Commun.* 51, 3501–3510. doi:10.1039/C4CC09596K
- Stassen, I., Burch, N., Talin, A., Falcaro, P., Allendorf, M., and Ameloot, R. (2017). An Updated Roadmap for the Integration of Metal-Organic Frameworks with Electronic Devices and Chemical Sensors. *Chem. Soc. Rev.* 46, 3185–3241. doi:10.1039/C7CS00122C
- Stavila, V., Talin, A. A., and Allendorf, M. D. (2014). MOF-based Electronic and Opto-Electronic Devices. *Chem. Soc. Rev.* 43, 5994–6010. doi:10.1039/C4CS00096J
- Su, J., Yuan, S., Wang, H.-Y., Huang, L., Ge, J.-Y., Joseph, E., et al. (2017). Redox-switchable Breathing Behavior in Tetrathiafulvalene-Based Metal-Organic Frameworks. *Nat. Commun.* 8 (2008), 1–8. doi:10.1038/s41467-017-02256-y
- Sumida, K., Rogow, D. L., Mason, J. A., McDonald, T. M., Bloch, E. D., Herm, Z. R., et al. (2012). Carbon Dioxide Capture in Metal-Organic Frameworks. *Chem. Rev.* 112, 724–781. doi:10.1021/cr2003272
- Sun, L., Campbell, M. G., and Dincă, M. (2016). Electrically Conductive Porous Metal-Organic Frameworks. *Angew. Chem. Int. Ed.* 55, 3566–3579. doi:10.1002/anie.201506219
- Wang, H.-Y., Cui, L., Xie, J.-Z., Leong, C. F., D'Alessandro, D. M., and Zuo, J.-L. (2017b). Functional Coordination Polymers Based on Redox-Active Tetrathiafulvalene and its Derivatives. *Coord. Chem. Rev.* 345, 342–361. doi:10.1016/j.ccr.2016.10.011
- Wang, H. Y., Ge, J.-Y., Hua, C., Jiao, C.-Q., Leong, C. F., Wu, Y., et al. (2017a). Photo- and Electronically Switchable Spin-Crossover Iron(II) Metal-Organic Frameworks Based on a Tetrathiafulvalene Ligand. *Angew. Chem. Int. Ed.* 56, 5465–5470. doi:10.1002/anie.201611824
- Wang, H.-Y., Su, J., Ma, J.-P., Yu, F., Leong, C. F., D'Alessandro, D. M., et al. (2019). Concomitant Use of Tetrathiafulvalene and 7,7,8,8-Tetracyanoquinodimethane within the Skeletons of Metal-Organic Frameworks: Structures, Magnetism, and Electrochemistry. *Inorg. Chem.* 58, 8657–8664. doi:10.1021/acs.inorgchem.9b01000
- Wang, H.-Y., Wu, Y., Leong, C. F., D'Alessandro, D. M., and Zuo, J.-L. (2015). Crystal Structures, Magnetic Properties, and Electrochemical Properties of Coordination Polymers Based on the Tetra(4-Pyridyl)-Tetrathiafulvalene Ligand. *Inorg. Chem.* 54, 10766–10775. doi:10.1021/acs.inorgchem.5b01803
- Weng, Y. G., Yin, W. Y., Jiang, M., Hou, J. L., Shao, J., Zhu, Q. Y., et al. (2020). Tetrathiafulvalene-Based Metal-Organic Framework as a High-Performance Anode for Lithium-Ion Batteries. *ACS Appl. Mater. Inter.* 12, 52615–52623. doi:10.1021/acsami.0c14510
- Yin, Z.-N., Li, Y.-H., Sun, Y.-G., Chen, T., Xu, J., Zhu, Q.-Y., et al. (2016). 3D Copper Tetrathiafulvalene Redox-Active Network with 8-fold Interpenetrating diamond-like Topology. *Inorg. Chem.* 55, 9154–9157. doi:10.1021/acs.inorgchem.6b01632
- Yuan, S., Feng, L., Wang, K., Pang, J., Bosch, M., Lollar, C., et al. (2018). Stable Metal-Organic Frameworks: Design, Synthesis, and Applications. *Adv. Mater.* 30 (1–35). doi:10.1002/adma.201704303
- Zhang, T., and Lin, W. (2014). Metal-organic Frameworks for Artificial Photosynthesis and Photocatalysis. *Chem. Soc. Rev.* 43, 5982–5993. doi:10.1039/C4CS00103F

Conflict of Interest: The authors declare that the research was conducted in the absence of any commercial or financial relationships that could be construed as a potential conflict of interest.

Publisher's Note: All claims expressed in this article are solely those of the authors and do not necessarily represent those of their affiliated organizations, or those of the publisher, the editors and the reviewers. Any product that may be evaluated in this article, or claim that may be made by its manufacturer, is not guaranteed or endorsed by the publisher.

Copyright © 2021 Gordillo, Benavides, Spalding and Saha. This is an open-access article distributed under the terms of the Creative Commons Attribution License (CC BY). The use, distribution or reproduction in other forums is permitted, provided the original author(s) and the copyright owner(s) are credited and that the original publication in this journal is cited, in accordance with accepted academic practice. No use, distribution or reproduction is permitted which does not comply with these terms.